JOURNAL OF GEOPHYSICAL RESEARCH, VOL. 103, NO. D24, PAGES 31,989–31,999, DECEMBER 27, 1998

Discriminating heavy aerosol, clouds, and fires during SCAR-B: Application of airborne multispectral MAS data

Michael D. King,[1] Si-Chee Tsay,[2] Steven A. Ackerman,[3] and North F. Larsen[4,5]

Abstract. A multispectral scanning spectrometer was used to obtain measurements of the reflection function and brightness temperature of smoke, clouds, and terrestrial surfaces at 50 discrete wavelengths between 0.55 and 14.2 μm. These observations were obtained from the NASA ER-2 aircraft as part of the Smoke, Clouds, and Radiation–Brazil (SCAR-B) campaign, conducted over a 1500 × 1500 km region of cerrado and rain forest throughout Brazil between August 16 and September 11, 1995. Multispectral images of the reflection function and brightness temperature in 10 distinct bands of the MODIS airborne simulator (MAS) were used to derive a confidence in clear sky (or alternatively the probability of cloud), shadow, fire, and heavy aerosol. In addition to multispectral imagery, monostatic lidar data were obtained along the nadir ground track of the aircraft and used to assess the accuracy of the cloud mask results. This analysis shows that the cloud and aerosol mask being developed for operational use on the moderate-resolution imaging spectroradiometer (MODIS), and tested using MAS data in Brazil, is quite capable of separating cloud, aerosol, shadow, and fires during daytime conditions over land.

1. Introduction

A knowledge of aerosol radiative properties and their variation in space and time is especially crucial to the understanding of the radiative forcing of climate. High-quality multispectral imagery, together with nadir-propagating lidar measurements, acquired from high-altitude aircraft or satellite platforms are the most efficient and reliable means of fulfilling these observational requirements. Between August 16 and September 11, 1995, the NASA ER-2 high-altitude research aircraft conducted 11 research flights throughout Brazil as part of the Smoke, Clouds, and Radiation–Brazil (SCAR-B) campaign. This aircraft was equipped with three primary sensors, the MODIS airborne simulator (MAS) [*King et al.*, 1996], the cloud lidar system (CLS) [*Spinhirne et al.*, 1982], and the airborne visible/infrared imaging spectrometer (AVIRIS) [*Vane et al.*, 1993]. The MAS was designed to obtain measurements that simulate those to be obtained from the moderate-resolution imaging spectroradiometer (MODIS), a sensor being developed for the Earth Observing System (EOS) AM-1 spacecraft [*King et al.*, 1995], scheduled for launch in fall 1998.

The strategy for SCAR-B included spaceborne remote sensing (polar orbiting and geosynchronous satellites), high-altitude remote sensing (NASA ER-2 at ~20 km), boundary layer in situ measurements (University of Washington C-131A and the INPE (Instituto de Pesquisas Espaciais) Bandeirante aircraft), ground-based measurements (Sun photometers, condensation nuclei counters, surface ozone concentration, and smoke aerosol samples collected on filters), and radiosondes [cf. *Kaufman et al.*, this issue (b)]. During SCAR-B the ER-2 was based in Brasília and deployed over vast areas of central and western Brazil. The main objectives of the ER-2 included (1) collecting cloud mask data for MODIS algorithm development, (2) collecting data for scale analysis at varying spatial resolutions, (3) collecting data for retrieving cloud and aerosol radiative and microphysical properties over various land surfaces, and (4) validating cloud mask retrievals using coincident monostatic CLS data onboard the aircraft.

Clouds are generally characterized by higher reflectance and lower temperature than the underlying surface. As such, simple visible and infrared window threshold approaches would appear to offer considerable skill in cloud detection. However, there are many surface conditions where this characterization of clouds is oversimplified and inappropriate, most notably over snow and sea ice surfaces. Additionally, some cloud types such as thin cirrus, low stratus at night, and small cumulus are difficult to detect because of insufficient contrast with the surface radiance (or reflectance). Cloud edges cause further difficulty because the instrument field of view will not always be completely cloudy or clear.

The 50 channel MAS offers an opportunity to explore and refine multispectral approaches to cloud detection, so many of these concerns can be mitigated, if not entirely eliminated. The intent of this paper is to describe the approach and algorithms used to detect clouds, shadows, fires, and heavy aerosol during daytime conditions in Brazil during austral spring. This represents a subset of all conditions and channels used to process global satellite data using MODIS. Preliminary results obtained from the ER-2 on two days during SCAR-B are presented to illustrate the results of applying these tests to a wide range of conditions. Finally, results of these retrievals are compared with nadir analysis of CLS data to verify the presence of cloud and heavy aerosol layers.

2. Instrumentation

The MAS is a cross-track scanning spectrometer that measures reflected solar and emitted thermal radiation in 50 nar-

[1]Earth Sciences Directorate, NASA Goddard Space Flight Center, Greenbelt, Maryland.
[2]Laboratory for Atmospheres, NASA Goddard Space Flight Center, Greenbelt, Maryland.
[3]Department of Atmospheric and Oceanic Sciences, University of Wisconsin, Madison.
[4]Geophysical Institute, University of Alaska, Fairbanks.
[5]Now at Raytheon STX Corp., Lanham, Maryland.

Copyright 1998 by the American Geophysical Union.

Paper number 98JD01043.
0148-0227/98/98JD-01043$09.00

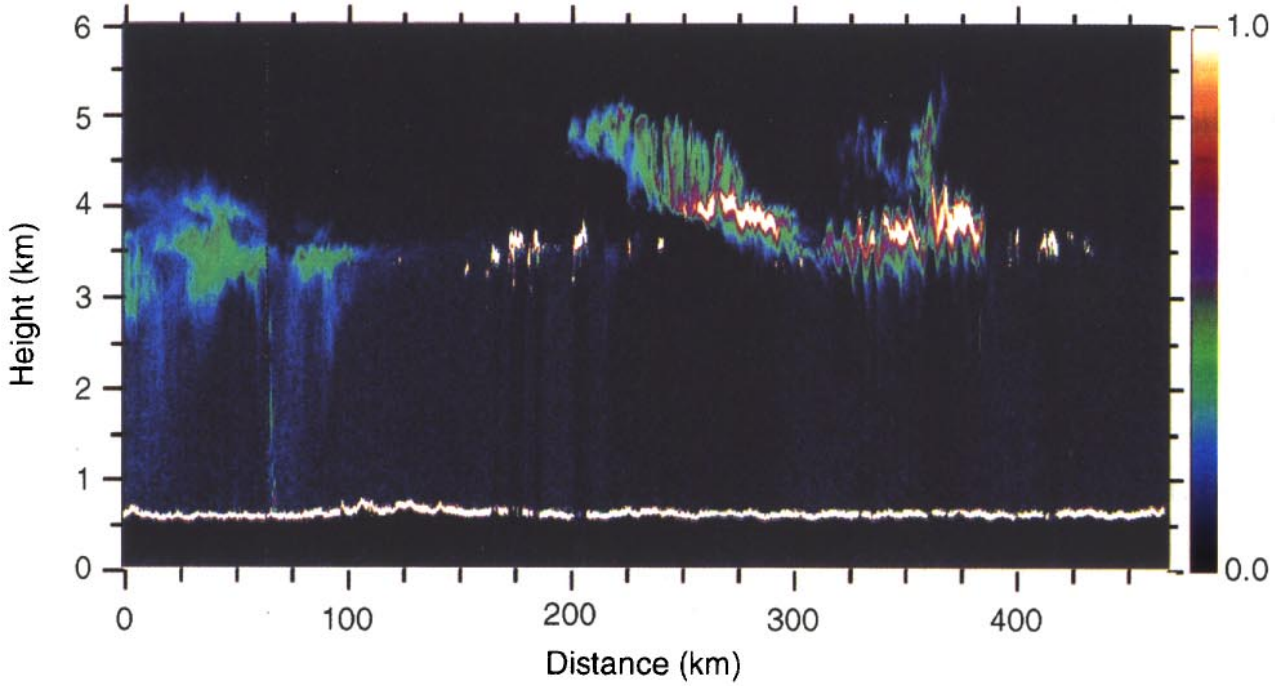

Plate 1. Cloud lidar system (CLS) observations of aerosol backscattering for the flight line from Alta Floresta to São Miguel do Araguaia on August 23, 1995 (1842:28 to 1917:06 UTC). Two prominent fires are evident between 225 and 390 km of this flight line, with the first fire producing heavy aerosol that punches through the inversion-capped boundary layer and the second producing gravity waves confined to the top of the boundary layer.

rowband channels between 0.55 and 14.2 μm. Flown aboard the NASA ER-2 aircraft, the MAS scans through nadir in a plane perpendicular to the velocity vector of the aircraft (cross track), with the maximum scan angle extending 43° on either side of nadir (86° full swath aperture). At a nominal ER-2 altitude of 20 km this yields a swath width of 37.2 km centered on the aircraft ground track. A total of 716 Earth-viewing pixels are acquired per scan at a scan rate of 6.25 Hz. Information provided by the aircraft inertial navigation system is used to adjust the timing of the digitizer, providing up to ±3.5° of roll compensation, in 0.03° increments. With each pixel having a 2.5 mrad (0.14°) instantaneous field of view, the spatial resolution at nadir is 50 m from the nominal aircraft altitude of 20 km.

Table 1 summarizes the band center and bandwidth characteristics as well as the dynamic range and main purpose of each MAS band used to detect clouds, aerosols, fires, and shadows during SCAR-B. Radiometric calibration of the shortwave (<2.5 μm) channels was obtained by observing laboratory standard integrating sphere sources on the ground before and after flight missions, while calibration of the infrared channels was performed by viewing two onboard blackbody sources once every scan. A detailed description of the optical, mechanical, electronics, and data acquisition system design of the MAS can be found in the work of *King et al.* [1996].

The CLS, a nadir-viewing, monostatic lidar system, which provides the true cloud top height as well as aerosol boundaries and the density structure of less dense clouds, was used to verify the performance of the cloud and aerosol mask for all 69 hours of colocated flights during SCAR-B. The CLS uses a

Table 1. Spectral and Radiometric Characteristics of all MAS Bands Used in the Aerosol, Cloud, and Fire Mask During SCAR-B (Daytime Land Conditions)

MAS Band	Equivalent MODIS Band	Central Wavelength μm	Spectral Resolution μm	R_{max}	T_{max} K	Primary Purpose
2	1	0.653	0.053	2.53	1613	low thick cloud, shadow, heavy aerosol
7	2	0.865	0.042	7.54	1429	low thick cloud, shadow
9	19	0.945	0.046	7.58	1336	shadow
15		1.889	0.051	5.04	754.5	thin cirrus
20	7	2.187	0.047	20.2	784.8	smoke aerosol, heavy aerosol
31	20	3.743	0.150	3.07	399.1	fire
32	21	3.901	0.167	32.07	511.2	fog, low cloud
45	31	11.022	0.543		379.0	fire, thin cirrus, fog, and low cloud
46	32	11.976	0.449		454.4	thin cirrus
49	35	13.723	0.600		701.4	high thick cloud

Maximum reflection function based on $\theta_0 = 22.5°$.

Nd:YAG laser, transmitting at 0.532 and 1.064 μm, and employs a 10 pulse per second firing rate. This results in vertical profiles of backscattering cross section being obtained at horizontal intervals of 20 m along the aircraft ground track and with a vertical sampling resolution of 7.5 m. This allows us to construct a detailed cloud and boundary layer aerosol topography and vertical structure in the nadir direction. A detailed description of the CLS is given by *Spinhirne et al.* [1982].

3. Cloud and Aerosol Mask

Development of the MAS cloud mask algorithm benefits from previous work to characterize global cloud cover using satellite observations [e.g., *Rossow*, 1989; *Rossow and Garder*, 1993; *Saunders and Kriebel*, 1988; *Stowe et al.*, 1991; *Wylie et al.*, 1994; *Strabala et al.*, 1994]. The MAS cloud mask indicates whether a given view of the Earth surface is unobstructed by clouds or optically thick aerosol and whether that clear scene is contaminated by shadow. The algorithm is divided into eight conceptual domains according to surface type (land, water, coastal, and desert) and solar illumination (daytime and nighttime). In this paper, for application to MAS data over Brazil during the austral spring we are concerned only with daytime land conditions, where daytime is defined for solar zenith angles $\theta_0 < 85°$. The United States Geological Survey 1 km land/sea tag file is used for land/water discrimination. Over land, ecosystem classification is based on the 10′ Olson World Ecosystems data set.

The threshold between a pixel being classified as cloudy or clear is sometimes ambiguous due to instrument noise and natural variability. To allow for imprecise measurements of the real world and to accommodate a wide variety of applications, the cloud mask is more than a simple yes/no decision. The cloud mask includes four levels of "confidence" with regard to whether a pixel is classified as clear. Confidence flags convey the strength of conviction in the outcome of the cloud mask algorithm tests for a given field of view (FOV). A confidence flag for each individual test, based on proximity to a threshold value, is assigned and used to derive a final quality flag determination for the pixel. The current scheme applies a linear interpolation between a low confidence clear (confidence = 0) and high confidence clear (confidence = 1) threshold for each spectral test. The final determination is a combination of the confidence indices of all applied tests.

Many cloud detection schemes used in the past are based on a single threshold for a given test. For example, if the visible reflectance over the ocean is greater than 6%, the pixel is classified as cloudy. It seems unrealistic and misleading to identify a pixel with 6.05% reflectance as cloudy, while a neighboring pixel with a reflectance of 5.95% is classified as noncloudy. The MAS cloud mask is designed to provide information on how much confidence a user can place in the result. The outcome of each spectral test is assigned a value between 0 and 1, representing increasing confidence of clear-sky conditions. Figure 1 is a graphical representation of how a confidence level is assigned for a spectral test. The abscissa represents the observation and the ordinate of the clear-sky confidence level. In this example, an observation greater than a value of γ is considered to have a high confidence of being clear and assigned a confidence value of 1. On the other hand, an observation with a value less than α is considered to be cloudy and assigned a confidence value of 0. Values between α and γ are assigned, based on a linear function, a confidence level between 0 and 1. The value of β represents a confidence level of 0.5. These high-confidence clear and cloud thresholds, γ and α, respectively, are determined from observations. Table 2 lists the MAS spectral tests that have been performed for all daytime land conditions during SCAR-B and identifies the high-confidence clear and cloudy threshold values used in each test. The thresholds used are based on previous studies and our own investigations [*Ackerman et al.*, 1998].

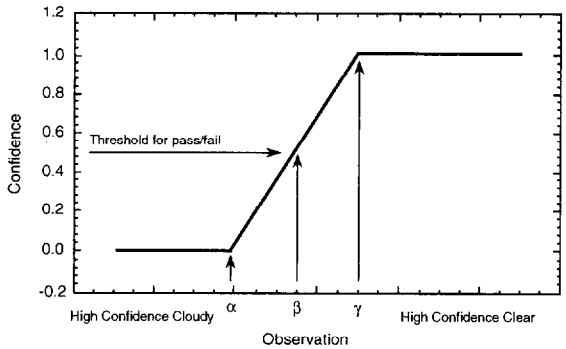

Figure 1. Graphical depiction of three thresholds used in cloud screening.

3.1. Combining Results From Individual Spectral Tests

The confidence levels of each spectral test must be combined to determine the final decision on whether a pixel is classified as clear or cloudy. Since several of the spectral tests are not independent of one another, the cloud mask algorithm first groups individual spectral tests. For example, for daytime over tropical forest conditions, stratocumulus clouds are likely to be detected by the visible reflectance test ($R_{0.65}$), the Global Environment Monitoring Index (GEMI) [*Pinty and Verstraete*, 1992], a nonlinear combination of $R_{0.65}$ and $R_{0.87}$ which was developed to correct for atmospheric contributions in relatively broadband AVHRR data, and the brightness temperature difference test ($T_{11} - T_{3.9}$). These same tests will likely miss the presence of thin uniform cirrus clouds, which would more likely be detected by infrared spectral tests (combinations of $T_{13.7}$, T_{11}, and T_{12}). Very thin cirrus clouds would best be detected by the 1.89 μm reflectance test ($R_{1.89}$), a test that yields very low reflectance values for clear sky as well as low level clouds in moist atmospheres. Because of the overlap in the sensitivity of certain spectral tests to the same type of cloud, each test is considered in one of four groups, as indicated in Table 2.

A minimum confidence is determined for each group as follows:

$$G_{j\ 1,N} = \min [F_i]_{i=1,m}, \tag{1}$$

where F_i is the confidence level of an individual spectral test, m is the number of tests in a given group, and N is the number of groups (four in this case). The final cloud mask (Q) is then determined from the product of the results from each group,

$$Q = \sqrt[N]{\prod_{j=1}^{N} G_j}. \tag{2}$$

This approach is clear-sky conservative in the sense that if any test is highly confident that the scene is cloudy ($F_i = 0$), the final clear sky confidence is 0.

Table 2. Threshold for Spectral Tests Applied to SCAR-B Data Set

Group	Test	Low Confidence Clear	Threshold	High Confidence Clear	Comment
I	$T_{13.7}$	219 K	220 K	221 K	high thick cloud
II	$T_{11} - T_{12}$	$a + 0.5$	a	$a - 0.5$	thin cirrus test; a is an empirical relation that depends on precipitable water
II	$T_{11} - T_{3.9}$	−18 K	−16 K	−14 K	fog and low thick cloud
III	$R_{0.65}$	0.29	0.27	0.25	thick cloud
III	$R_{0.87}/R_{0.65}$				thick cloud (GEMI variant test)
IV	$R_{1.89}$	0.03	0.025	0.02	thin cirrus

Group	Test	Low Confidence Shadow	Threshold	High Confidence Shadow	Comments
Shadow	$R_{0.887}/R_{0.65}$	0.85	0.90	0.95	both of these tests mush yield shadow for pixel to be identified as shadow
Shadow	$R_{0.95}$		<0.12		
Heavy aerosol	$R_{2.19}$		<0.20		both of these tests mush yield heavy aerosol for pixel to be identified as such
Heavy aerosol	$R_{0.65}$		$>0.04 + R_{2.19}/2$		
Fire	$T_{3.7}$		>350 K		both of these tests identify fire
Fire	$T_{3.7} - T_{11}$		>10 K		if fire, heavy aerosol bit is turned on

3.2. Heavy Aerosol Flag

An atmosphere laden with heavy aerosol may result in a low-confidence clear scene. Certain simple tests may be constructed which can indicate that the FOV is contaminated with an aerosol and not a cloud. The thresholds are conservative in that thin aerosol layers are often flagged as clear. Figure 2 shows the logical flowchart of the heavy aerosol flag, based largely on the work of *Kaufman et al.* [1997]. The principle behind this technique is the observation that the reflectance at 2.1 μm is largely unaffected by heavy aerosol (except dust) and can hence be used to detect dark surface targets during the day. Using observed correlations between surface reflectance at 0.66 and 2.19 μm, Kaufman et al. concluded that $R_{0.66}$ can be well approximated by $R_{2.19}/2$.

3.3. Detection of Cloud Shadows

The detection of cloud shadows is a problem that has not been addressed adequately in the literature. Clear-sky scenes that are potentially affected by shadows can theoretically be computed given the viewing geometry, solar azimuth and zenith angles, cloud edges distribution, and cloud top altitude. This approach requires too much computer time to run operationally, and all necessary input information (namely, cloud top altitude) is not available at the time the cloud mask is executed. Therefore, as with clouds, solar reflectance tests are used in the cloud shadow detection algorithm.

The cloud mask algorithm checks for shadows whenever a highly confident clear scene is identified. Shadow detection is based on reflectance at 0.95, 0.87, and 0.65 μm. A shadow is identified when $R_{0.95} < 0.12$ and $R_{0.87}/R_{0.65} > 0.9$.

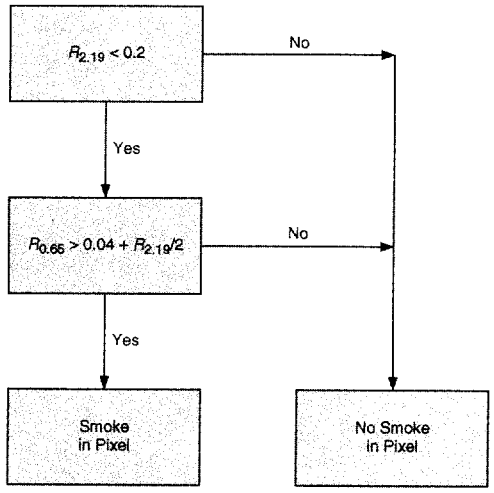

Figure 2. Schematic diagram for determining the presence of heavy aerosol over land during daytime.

3.4. Detection of Fires

The detection of fires is straightforward from MAS because of the large dynamic range of bands 31 and 45 (compare Table 1). Even if T_{11} cannot be determined due to extremely high temperature, and therefore saturation ($T_{11} > 379$ K), the thermal emission at 3.74 μm permits hot fires to be detected. Hot fires are detected when $T_{3.7} > 350$ K and $T_{3.7} - T_{11} > 10$ K. Although the 2.19 μm radiance is sensitive to fires due to the enhanced thermal emission at this wavelength for hot fires, this channel has yet to be incorporated in the fire mask using MAS data.

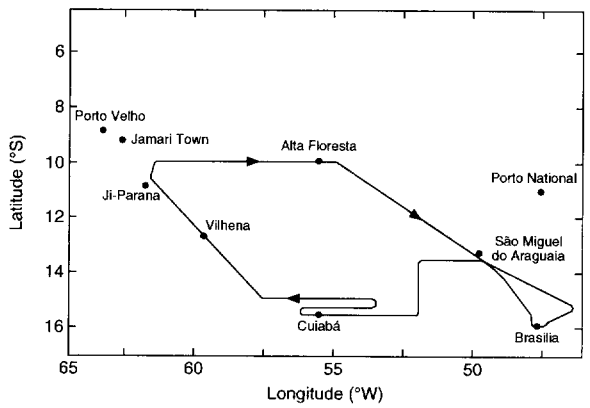

Figure 3. Ground track of the ER-2 on August 23, 1995.

4. Results From Observations

During SCAR-B the ER-2 acquired 69 hours of MAS and CLS data during 11 research flights between August 16 and September 11, 1995. These flights included repeated flights over an extensive network of ground-based Sun/sky radiometers throughout Brazil [*Holben et al.*, 1998]. In what follows we will describe results obtained from the ER-2 on two of these flights and demonstrate the performance of the cloud and aerosol mask over terrestrial land surfaces during the day.

4.1. August 23, 1995

On August 23 the ER-2 overflew the Cuiabá Sun photometer site during a mapping grid that consisted of three flight legs 300 km in length spaced 35 km apart and parallel, in which the aerosol concentration was relatively low. Following this portion of the flight, the ER-2 headed 650 km northwest to overfly a Sun photometer site near Ji-Parana in Rondonia. The pilot reported a tremendous amount of smoke and was unable to see the ground throughout much of this flight line. He also observed smoke rising and spreading out uniformly in all directions, with an extremely flat upper boundary associated with a strong inversion layer. The ER-2 then flew one flight line 700 km in length which went over the Sun photometer site at Alta Floresta. The pilot reported two very large fires between 1858 and 1911 UTC on his return leg to Brasília. Figure 3 illustrates the ER-2 ground track for this mission.

Plate 1 shows measurements obtained by the CLS at 1.064 μm along the nadir track of the ER-2 from Alta Floresta to São Miguel do Araguaia, prior to descending to land at Brasília. These data show that this entire 470 km region was covered by a thick aerosol layer confined below a temperature inversion at ~3.5 km, with little change in the depth of the boundary layer over this great distance. Also evident in this figure are smoke clouds punching through the inversion-capped boundary layer and gravity waves confined to the top of the boundary layer, located between 225 and 390 km of this flight line.

The MAS acquired reflected solar and emitted thermal radiation measurements in 50 narrowband channels, 10 of which were used to test the cloud, aerosol, fire, and shadow mask outlined in section 3 (compare Table 1). Figure 4 shows images of a haze-filled boundary layer 205 km in length over northeastern Mato Grosso some 560–760 km NW of Brasilia, where the ER-2 is flying from top to bottom down these images. These images correspond to the last 205 km portion of the lidar image shown in Plate 1. MAS visible and near-infrared channels can readily be used to detect smoke and haze, burn scars, river beds, and regrowth. The left-hand panel (0.65 μm) is especially sensitive to scattering by smoke and haze, with dark surface features being very difficult to discern through the thick haze. At the upper portion of the image there are two prominent smoke plumes from active fires, as reported by the pilot. The middle panel (0.87 μm) is largely insensitive to aerosol scattering and is therefore quite transparent to haze. The surface is bright throughout most of this largely forested region, and shadows stand out much more than at 0.65 μm. At 2.19 μm (right-hand panel), old growth forest is dark, but burn scars and recent regrowth are bright, as is typical of cities with pavement and buildings.

These three channels give only a hint at the wealth of information available in 50 channel high spatial resolution data. Plate 2 shows a false-color composite image of this scene, together with images of the cloud and shadow mask and aerosol and fire mask applied to this scene. The false-color image was constructed by contrast stretching and combining three spectral bands into one 24 bit image, where the spectral bands were assigned to red, green, and blue (RGB) 8 bit display channels. For this scene, the RGB assignment was 2.19 μm (red), 0.87 μm (green), and 0.65 μm (blue), corresponding to the same channels presented in Figure 4. In this manner the haze and smoke appear blue, burn scars brown, unburned vegetation green, clouds white, and fires red.

The middle panel in Plate 2 represents the results of the cloud and shadow mask applied to this scene. As discussed in the previous section, the cloud mask assigns four levels of clear sky "confidence" to each pixel. In this panel, the high-confidence clear-sky image on which the cloud and shadow masks are superimposed is the MAS reflectance in band 2 (0.65 μm). The cloud mask results are designated as cloudy, with a confidence $Q < 1\%$, probably clear ($Q > 66\%$), confident clear ($Q > 95\%$), and high-confidence clear ($Q > 99\%$). Comparing the cloud and shadow mask results to the false-color image on the left in Plate 2, it appears that the clouds and shadows in the bottom portion of the image are being classified quite accurately. In the top portion of this image, on the other hand, the smoke from the two great fires is being partly confused as probably clear and cloudy. The cloudy regions of the second fire are in part correctly identified, but those in the upper fire are being misidentified as cloud. This is a result of the rather large reflectance observed at 0.87 μm (compare Plate 2).

The heavy aerosol and fire tests were also applied to this scene, with apparently good success. By comparing Figure 4 with the tests applied to heavy aerosol, described in Table 2, it is quite apparent that the extremely large smoke plumes arising from the two great fires in the top portion of the image are completely transparent at 2.19 μm. This would not be the case for clouds unless they had especially large cloud droplets [*Nakajima and King*, 1990; *King et al.*, 1992]. The hot fire at 125 km is properly identified as a fire due to the hot thermal signature arising at 3.74 and 11.02 μm (images not shown).

4.2. September 4, 1995

On September 4, 1995, the ER-2 flew a flux ground track near Bolivia, from Cuiabá to Rondonia, followed by several flight lines over Jamari Town and Darold Ward's surface site. The flight line from Cuiabá to Vilhena was coordinated with the C-131A, which then broke off to land and refuel. Figure 5 illustrates the ER-2 ground track for this mission, where the ER-2 once again took off from Brasilia, located on a central plateau, and then flew over the low-land Sun photometer site in Cuiabá before flying the 800 km flight track to Porto Velho, Rondonia.

Plate 3 shows measurements obtained by the CLS along the nadir track of the ER-2 flight line from Cuiabá to Porto Velho. These data clearly show that this entire 965 km region was covered by a thick haze layer ~4.5 km thick, with very little change in the depth of the boundary layer over this great distance. Also evident in this figure are capping smoke clouds at the top of the inversion-capped boundary layer between 300 and 350 km, near the Cuiabá end of the flight line.

Figure 6 shows MAS images of a haze-filled boundary layer 205 km in length over western Mato Grosso and southern Rondonia. The ER-2 is again flying from top to bottom down these images, which correspond to the central portion (545–

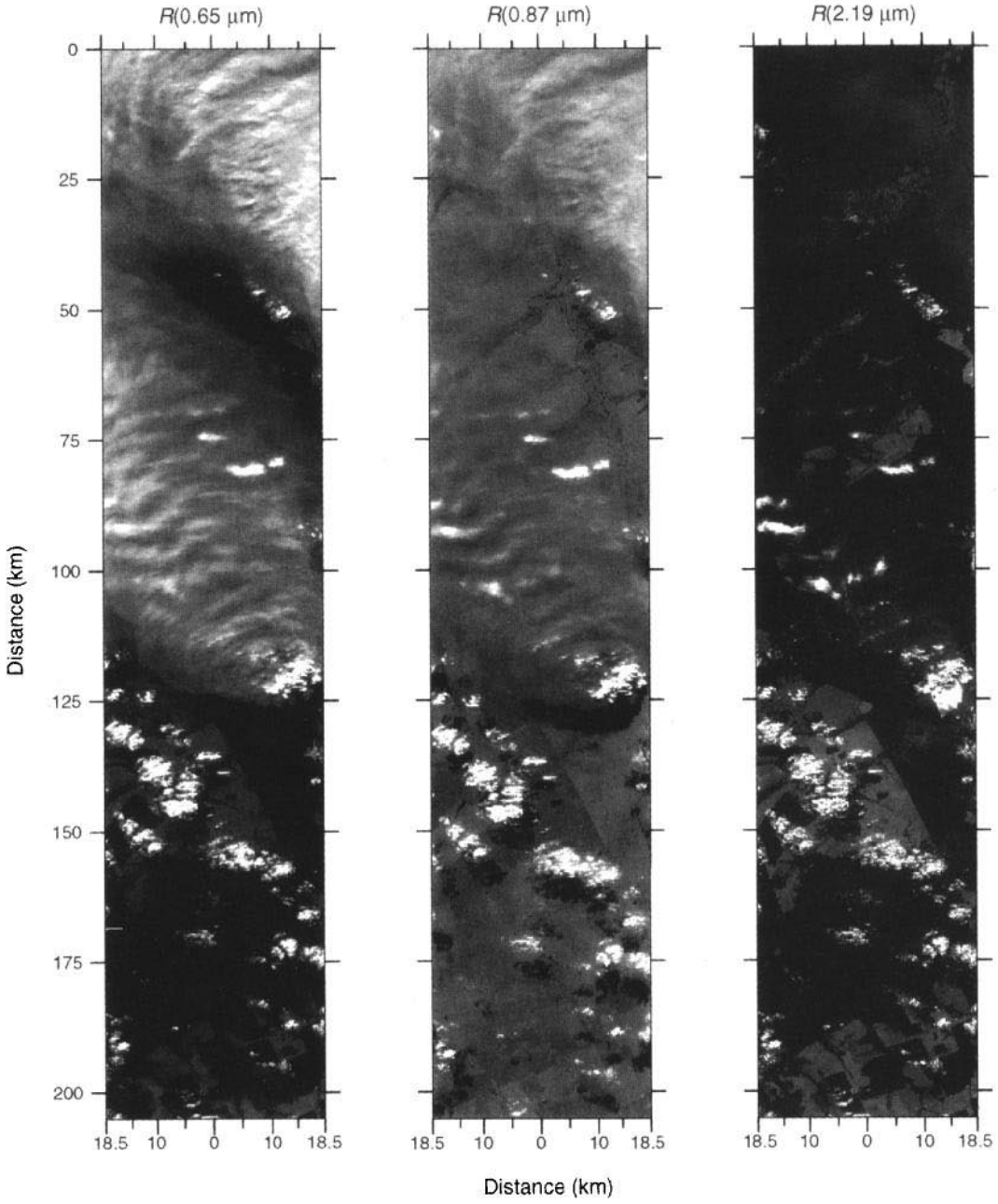

Figure 4. MODIS airborne simulator (MAS) images of the final 205 × 37 km section of the flight line from Alta Floresta to São Miguel do Araguaia on August 23, 1995 (5668 scan lines between 1901:59 and 1917:06 UTC). At 0.65 μm it is difficult to see the ground due to the heavy smoke and aerosol from extensive biomass burning. At 0.87 μm, on the other hand, surface reflectance is high and haze transparent, except where the ground has already been burned and is dark from burn scars or shadows. At 2.19 μm the burn scars are again quite reflective, as is often the case over pavement in cities, and the clouds and fires are readily apparent.

750 km) of the lidar image shown in Plate 3. Once again, the MAS visible and near-infrared channels can be used to detect smoke and haze, burn scars, clear cut roads (especially in Rondonia toward the latter third of the image), and regrowth. The panel on the left (0.65 μm) is again sensitive to scattering by smoke and haze, with ground features difficult to discern through the haze, but there is also evidence of a scan angle dependence to the reflected radiance, with the off-nadir pixels exhibiting enhanced scattering over pixels at nadir. This scene contains only two small fires and is primarily dominated by aged aerosol. The middle panel (0.87 μm) is largely insensitive to aerosol backscattering, being largely transparent to haze, and is dominated by bright reflectance from undisturbed vegetation. Clear-cut forests, river valleys with sparse vegetation, and recently burnt vegetation are generally dark throughout the image. At 2.19 μm (right-hand panel), old growth forest is quite dark, but burn scars and recent regrowth stand out in stark contrast as bright features in the image.

Plate 4 shows a composite false-color image constructed from the 2.19 μm (red), 0.87 μm (green), and 0.65 μm (blue) bands of MAS. This false-color image brings out the stark contrast between the undisturbed forest (green), heavy aerosol

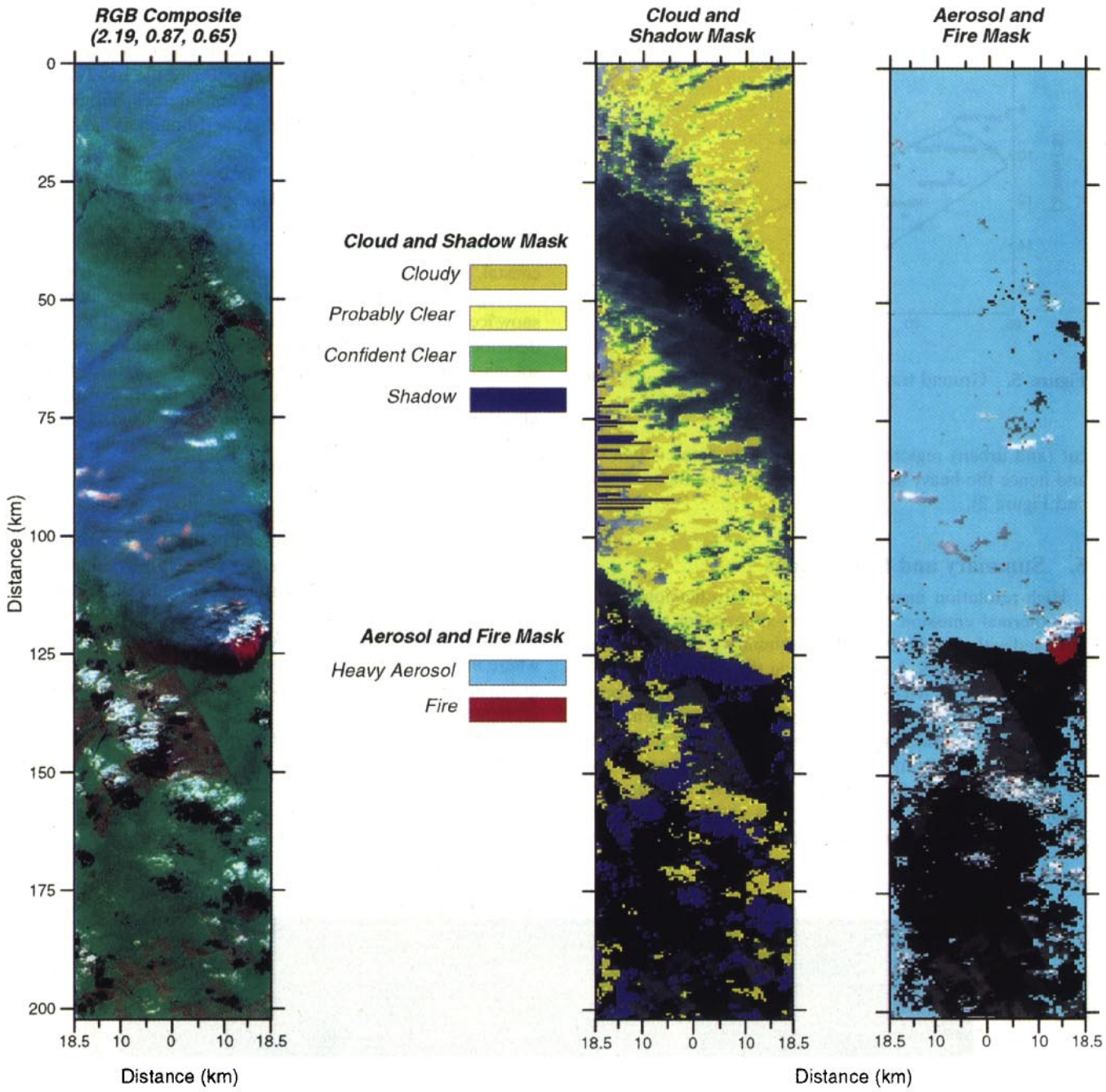

Plate 2. Composite image (left) of smoke, burn scars, and unburned vegetation in Mato Grosso on August 23, 1995. The RGB assignment is red (2.19 μm), green (0.87 μm) and blue (0.65 μm) and is based on the individual channels shown in Figure 4. The middle panel is the resultant cloud and shadow mask, and the final panel is the heavy aerosol and fire mask. Most of the scene is classified as heavy aerosol, as expected. The background image on which the cloud and aerosol mask are overlaid is the MAS reflectance image at 0.65 μm.

(bluish tint, especially noticeably at the higher slant path angles near the edge of the image), and clear-cut forest and burn scars (magenta). The cloud mask (middle panel) is again overlain on the 0.65 image for high-confidence clear conditions. This retrieval correctly identifies the two small fires present in this scene, but the subsequent shadow mask overestimates the presence of shadow, especially on the forward scattering side of the image (relative azimuth angle $\phi = 23°$). Many false results are observed, including burn scars and regions of excessive forward scattering, since the heading of this flight line (323°) leads to scans close to the principle plane of the Sun. The two horizontal bands in the image at 107 and 137 km arise from bad data at 3.7 and/or 11 μm. Were the data needed for the test missing, the cloud mask would not have been run, but there are no checks for "bad" data.

The heavy aerosol mask was also run on this scene (right-hand panel), and the results correctly find the scene to be nearly completely covered by heavy aerosol, commensurate with our expectations from the lidar data presented in Plate 3. Areas where heavy aerosol was not identified, most notably the clear-cut forest in Rondonia, are associated with regions in which the heavy aerosol mask was not applied. For these clear-

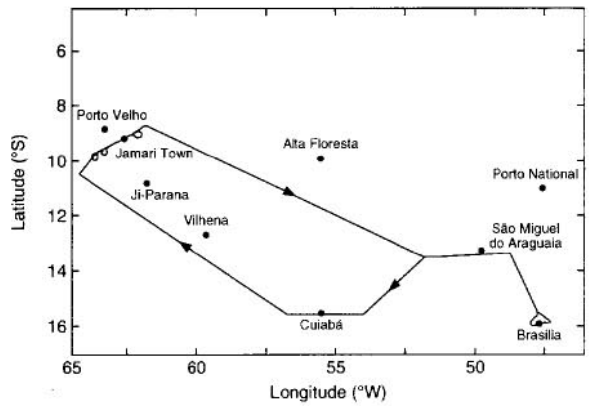

Figure 5. Ground track of the ER-2 on September 4, 1995.

cut (and urban) regions, $R_{2.19}$ is typically greater than 0.20, and hence the heavy aerosol flag is not set (compare Table 2 and Figure 2).

5. Summary and Conclusions

High-resolution images of the spectral reflection function and thermal emission of the Earth-atmosphere system were obtained with the MODIS airborne simulator (MAS) operated from the NASA ER-2 aircraft during the intensive field component of the SCAR-B experiment, conducted over central and western Brazil between August 16 and September 11, 1995. Multispectral images of the reflection function and brightness temperature at 10 wavelengths between 0.65 and 13.72 μm were used to derive the probability of clear sky (or cloud), shadows over the ground, fires, and heavy aerosol on two days (August 23 and September 4), where each image was approximately 37 km in width and 205 km in length. On both of these days, as was the case throughout the dry season in Brazil, the cloud lidar system (CLS) onboard the ER-2 showed that the heavy aerosol resulting from biomass burning was largely confined to an inversion-capped boundary layer typically 3–5 km in depth.

As a test of the MODIS cloud mask algorithm [*Ackerman et al.*, 1997, 1998], being developed for operational determination of clouds, shadows, and heavy aerosol from MODIS for 10 conceptual domains according to surface type (land, water, coastal, desert, and snow/ice) and solar illumination (daytime and nighttime), a MAS version of the algorithm (without the snow/ice surface category) has been developed. This paper describes the application of this version of the cloud and aerosol mask for daytime conditions over land, as applied to biomass burning aerosol, clouds, and fires in Brazil. For this application the MAS cloud mask can be summarized as follows:

1. Determine if the pixel is a land or water scene. If land, determine the ecosystem type; if water, determine whether the pixel is in a Sun glint region.
2. Apply appropriate single FOV masking tests (compare Table 2) and set initial unobstructed FOV determination for a given domain. Initial confidence flag (F_i) is assigned for each test result, depending on its position relative to the threshold.
3. The single FOV cloud test results are grouped and the minimum of each group determined ($G_{i=1,N} = \min [F_i]_{i=1,m}$), where m represents the number of individual tests in a given group and N the four groups used for daytime land conditions (compare Table 2).
4. The group minimums are then multiplied together and the N^{th} root taken, producing the clear-sky confidence mask (Q).
5. Check for cloud shadow on the ground.
6. Check for heavy aerosol and fire.

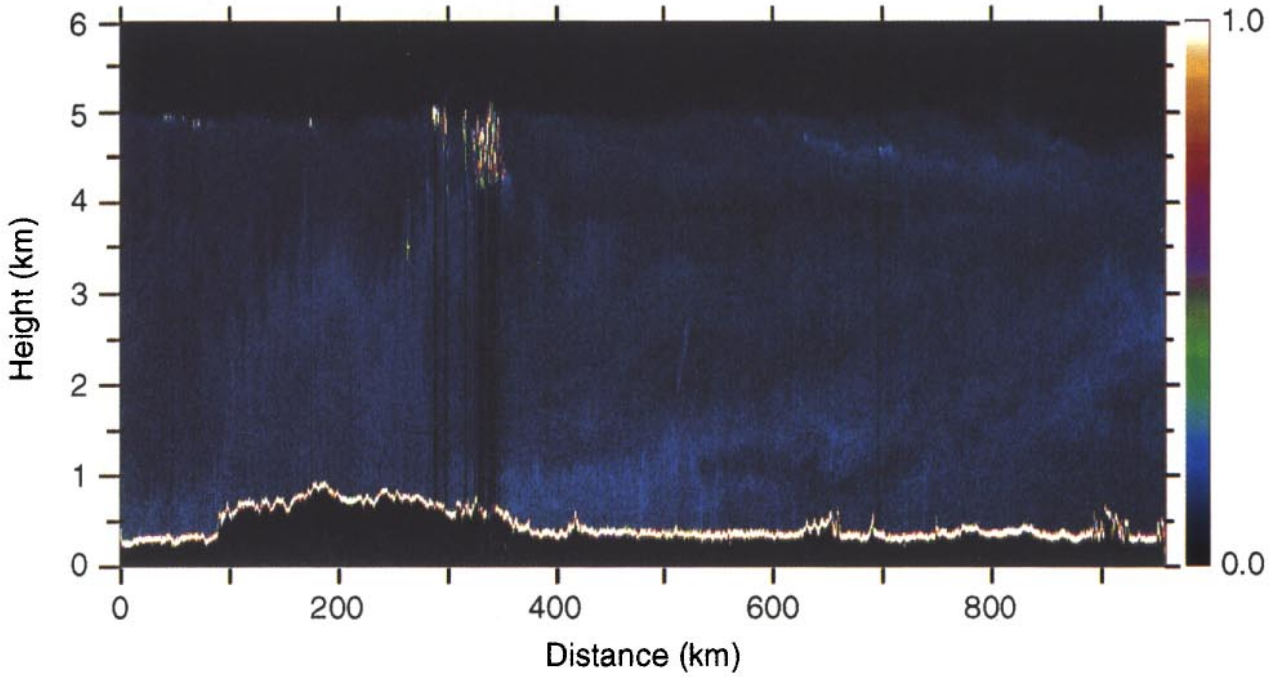

Plate 3. CLS observations of aerosol backscattering for the flight line from Cuiabá to Porto Velho on September 4, 1995 (1507:10 to 1625:23 UTC). The well mixed and hazy boundary layer is clearly evident in this plate.

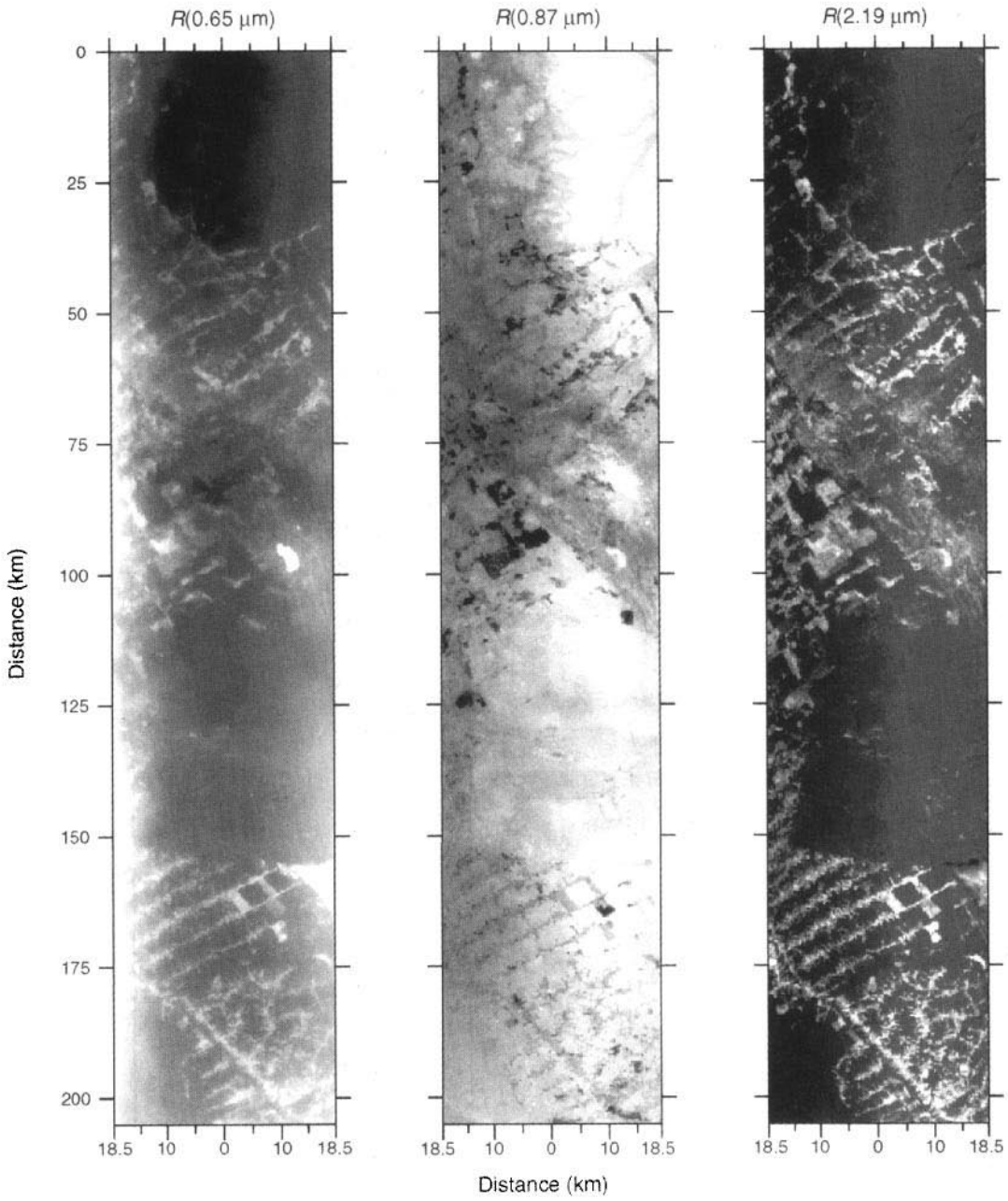

Figure 6. MAS images of a central 205 × 37 km section of the flight line from Cuiabá to Vilhena on September 4, 1995 (5668 scan lines between 1552:43 and 1607:50 UTC). At 0.65 μm it is difficult to see the ground due to the heavy smoke and aerosol from extensive biomass burning, but the clear-cut roads in Rondonia are apparent as enhanced reflectance in the lower third of the image. At 0.87 μm, on the other hand, surface reflectance from vegetation is high and haze transparent, except where the ground has been burned or cleared. At 2.19 μm the burn scars and clear-cut forests are again quite reflective.

One of the unique aspects of this experiment was the ability to coordinate airborne monostatic lidar measurements with nearly simultaneous multispectral radiance measurements obtained from the same platform. This use of multiple sensors provided us the opportunity to compare the remote-sensing-derived cloud and aerosol mask with extremely sensitive lidar measurements, at least along the nadir track of the ER-2 aircraft.

Our comparisons between remote-sensing-derived values of the heavy aerosol and fire mask (Plates 2 and 4) and high-resolution imagery and monostatic lidar measurements demonstrate that the aerosol mask properly detects heavy aerosol over land during daytime in Brazil, at least during the biomass burning season. As presently implemented, the heavy aerosol mask is not applied when the reflection function at 2.19 μm ($R_{2.19}$) exceeds 0.2. Hence for deforested areas and urban/suburban environments, conditions for which $R_{2.19}$ is typically larger than 0.2, the heavy aerosol mask is not tested or applied. In the optically thinner regions of the MAS scene, heavy aerosol is more likely to be detected off nadir than at nadir, due largely to the fact that the heavy aerosol thresholds are not view angle dependent, as they should be. At least for the

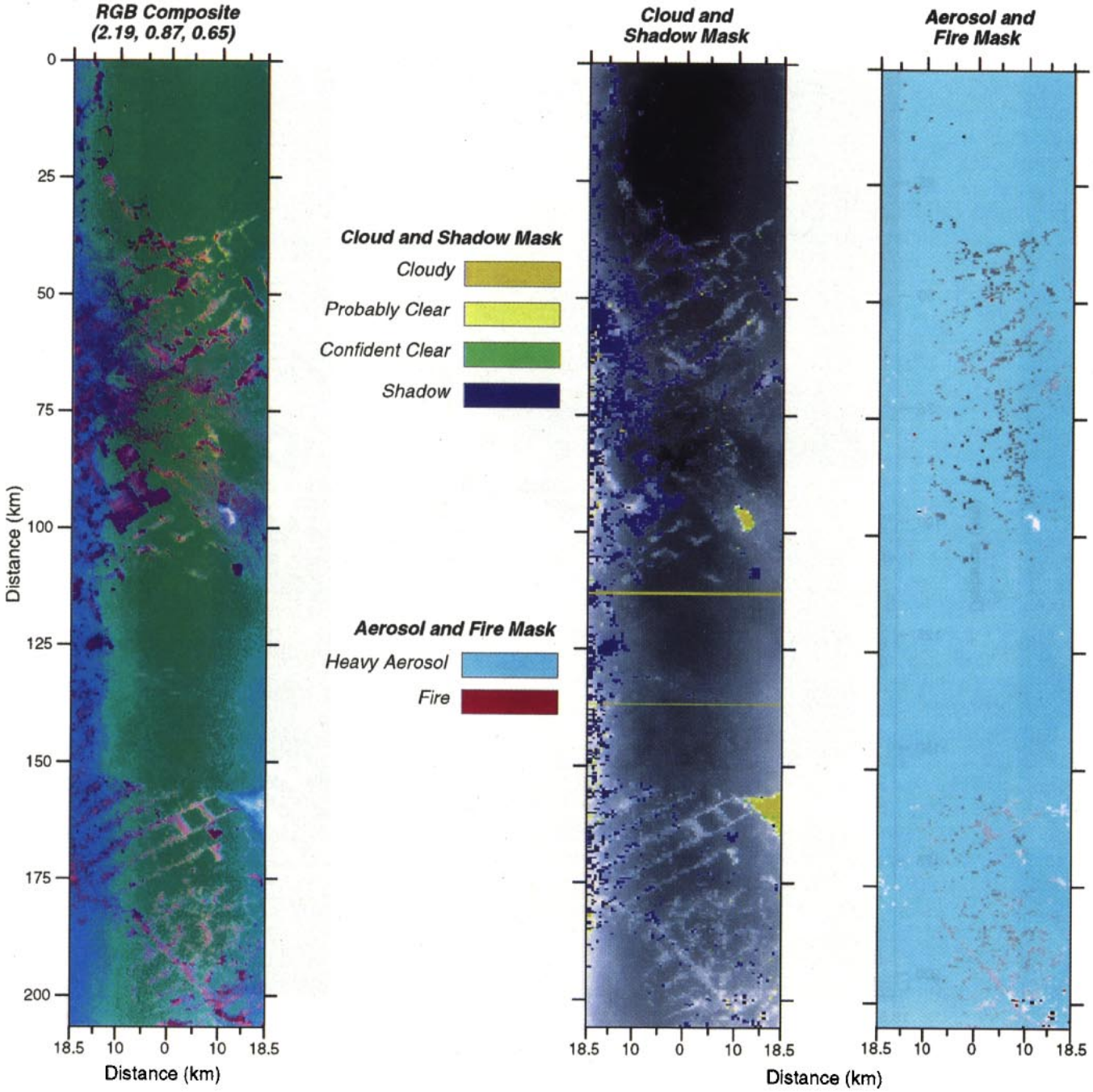

Plate 4. Composite image (left) of smoke, burns, and unburned vegetation in Mato Grosso on September 4, 1995. The RGB assignment is red (2.19 μm), green (0.87 μm) and blue (0.65 μm) and is based on the individual channels shown in Figure 6. The middle panel is the resultant cloud and shadow mask, and the final panel is the fire and heavy aerosol mask. Most of the scene is classified as heavy aerosol, as expected, with only a few clouds. The background image on which the cloud and aerosol mask are overlaid is the MAS reflectance image at 0.65 μm.

spatial resolution of MAS (50 m at nadir) it is extremely easy to detect hot fires due to their strong thermal contrast to their surroundings. In our application of the fire mask, described above, we used the 3.74 and 11.02 μm bands of MAS, though we could very well have utilized the 2.19 or 3.90 μm bands, as implemented by *Kaufman et al.* [this issue].

The cloud mask also appears to work well in Brazil, except under extremely thick aerosol conditions for which the reflection function at 0.87 μm ($R_{0.87}$) exceeds our expectations for aerosol scattering (compare Plate 2). Under these optically thick conditions the thickest part of the aerosol layer is misidentified as cloud ("cumulus"). The isolated cumulus mediocris clouds in Plate 2 and the fire-induced cumulus congenitus clouds in Plate 4 appear to be properly identified as cloud. Furthermore, our results for the shadow mask appear to work best for cloud shadows on the ground and not very well for shadows of upper clouds on lower clouds (not shown in this paper). Areas where the shadow mask has its greatest difficulties are burn scars, which are naturally quite dark at 0.87 μm, especially in the forward scattering direction (compare Plate 4).

All MAS flights for SCAR-B have been processed to level 1b (calibrated and geolocated radiances) using final radiometric and spectral calibration, with data sent to the Langley Research Center DAAC (Distributed Active Archive Center). In addition, browse images, a MAS data user's guide, software for unpacking and interpreting the data, and information on where and how to obtain data, are accessible via World Wide Web (http://ltpwww.gsfc.nasa.gov/MAS). SCAR-B involved satellite remote sensing, high-altitude and boundary layer aircraft measurements, and ground-based remote sensing and in situ measurements. It is an unprecedented data set with many science results anticipated following more extensive analysis in the future.

Acknowledgments. The research reported in this article was supported by the MODIS science team, the EOS Project Science Office, and NASA's Radiation Science Program. One of us (SAA) was supported by NASA contract NAS5-31367 to the University of Wisconsin. We would like to express our appreciation to James D. Spinhirne, Goddard Space Flight Center, for providing the CLS data used in this paper, and Paul Hubanks, Research and Data Systems Corp., for processing all MAS data to level 1b and maintaining the World Wide Web site so useful to the scientific community.

References

Ackerman, S., K. Strabala, P. Menzel, R. Frey, C. Moeller, L. Gumley, B. Baum, C. Schaaf, and G. Riggs, Discriminating clear-sky from cloud with MODIS: Algorithm Theoretical Basis Document (MOD35), 125 pp., NASA Goddard Space Flight Cent., (http://eospso.gsfc.nasa.gov/atbd/modistables.html), 1997.

Ackerman, S. A., K. I. Strabala, W. P. Menzel, R. A. Frey, C. C. Moeller, and L. E. Gumley, Discriminating clear sky from clouds with MODIS, *J. Geophys. Res.*, in press, 1998.

Holben, B. N., et al., AERONET—A federated instrument network and date archive for aerosol characterization, *Remote Sens. Environ.*, in press, 1998.

Kaufman, Y. J., A. Wald, L. A. Remer, B. C. Gao, R. R. Li, and L. Flynn, The MODIS 2.1 μm channel—Correlation with visible reflectance for use in remote sensing of aerosol, *IEEE Trans. Geosci. Remote Sens.*, *35*, 1286–1298, 1997.

Kaufman, Y. J., R. G. Kleidman, and M. D. King, SCAR-B fires in the tropics: Properties and their remote sensing from EOS-MODIS, *J. Geophys. Res.*, this issue (a).

Kaufman, Y. J., et al., Smoke, Clouds, and Radiation-Brazil (SCAR-B) experiment, *J. Geophys. Res.*, this issue (b).

King, M. D., D. D. Herring, and D. J. Diner, The Earth Observing System (EOS): A space-based program for assessing mankind's impact on the global environment, *Opt. Photon. News*, *6*, 34–39, 1995.

King, M. D., Y. J. Kaufman, W. P. Menzel, and D. Tanré, Remote sensing of cloud, aerosol, and water vapor properties from the Moderate Resolution Imaging Spectrometer (MODIS), *IEEE Trans. Geosci. Remote Sens.*, *30*, 2–27, 1992.

King, M. D., et al., Airborne scanning spectrometer for remote sensing of cloud, aerosol, water vapor and surface properties, *J. Atmos. Oceanic Technol.*, *13*, 777–794, 1996

Nakajima, T., and M. D. King, Determination of the optical thickness and effective particle radius of clouds from reflected solar radiation measurements, I, Theory, *J. Atmos. Sci.*, *47*, 1878–1893, 1990.

Pinty, B., and M. M. Verstraete, GEMI: A non-linear index to monitor global vegetation from satellites, *Vegetation*, *101*, 15–20, 1992.

Rossow, W. B., Measuring cloud properties from space, A review, *J. Clim.*, *2*, 201–213, 1989.

Rossow, W. B., and L. C. Garder, Cloud detection using satellite measurements of infrared and visible radiances for ISCCP, *J. Clim.*, *6*, 2341–2369, 1993.

Saunders, R. W., and K. T. Kriebel, An improved method for detecting clear sky and cloudy radiances from AVHRR data, *Int. J. Remote Sens.*, *9*, 123–150, 1988.

Spinhirne, J. D., M. Z. Hansen, and L. O. Caudill, Cloud top remote sensing by airborne lidar, *Appl. Opt.*, *22*, 1564–1571, 1982.

Stowe, L. L., E. P. McClain, R. Carey, P. Pellegrino, G. Gutman, P. Davis, C. Long, and S. Hart, Global distribution of cloud cover derived from NOAA/AVHRR operational satellite data, *Adv. Space Res.*, *11*, 51–54, 1991.

Strabala, K. I., S. A. Ackerman, and W. P. Menzel, Cloud properties inferred from 8–12 μm data, *J. Appl. Meteorol.*, *33*, 212–229, 1994.

Vane, G., R. O. Green, T. G. Chrien, H. T. Enmark, E. G. Hansen, and W. M. Porter, The Airborne Visible/Infrared Imaging Spectrometer (AVIRIS), *Remote Sens. Environ.*, *44*, 127–143, 1993.

Wylie, D. P., W. P. Menzel, H. M. Woolf, and K. I. Strabala, Four years of global cirrus cloud statistics using HIRS, *J. Clim.*, *7*, 1972–1986, 1994.

S. A. Ackerman, Department of Atmospheric and Oceanic Sciences, University of Wisconsin, Madison, WI 53706.

M. D. King, Earth Science Directorate, NASA Goddard Space Flight Center, Code 900, Greenbelt, MD 20771. (e-mail: king@climate.gsfc.nasa.gov)

N. F. Larsen, Raytheon STX Corp., Lanham, MD 20706.

S.-C. Tsay, Laboratory for Atmospheres, NASA Goddard Space Flight Center, Greenbelt, MD 20771.

(Received September 30, 1997; revised March 18, 1998; accepted March 20, 1998.)